Astron. Astrophys. 328, 399–408 (1997)

ASTRONOMY
AND
ASTROPHYSICS

Resonance and chaos

II. Exterior resonances and asymmetric libration

O.C. Winter[1,2] **and C.D. Murray**[2]

[1] Grupo de Dinâmica Orbital e Planetologia, Campus Guaratinguetá, UNESP, CP 205, CEP 12500-000, Guaratinguetá, São Paulo, Brazil
[2] Astronomy Unit, Queen Mary and Westfield College, University of London, Mile End Road, London E1 4NS, UK

Received 23 September 1996 / Accepted 18 December 1996

Abstract. The motion of a test particle in the vicinity of exterior resonances is examined in the context of the planar, circular, restricted three-body problem. The existence of asymmetric periodic orbits associated with the $1 : n$ resonances (where $n = 2, 3, 4, 5$) is confirmed; there is also evidence of asymmetric resonances associated with larger values of n. A detailed examination of the evolution of the family of orbits associated with the 1:2 resonance shows the sequence that leads to asymmetric libration. On the basis of numerical studies of the phase space it is concluded that the existence of asymmetric libration means that the region exterior to the perturbing mass is more chaotic than the interior region. The apparent absence of 'particles' in $1 : n$ resonances in the solar system may reflect this inherent bias.

Key words: chaos – dynamics – asteroids

1. Introduction

In a previous paper (Winter & Murray 1996, henceforth referred to as Paper I) we analysed a variety of models for resonant libration at the location of the first-order, interior resonances in the context of the planar, circular restricted three-body problem. In Paper I we compared the analytical results with data derived from extensive integrations of the full equations of motion for a reduced mass of 10^{-3}. We demonstrated that, contrary to theoretical predictions, there is no extensive overlap of adjacent resonances at low eccentricities. We showed how the phenomenon of apocentric libration arises from the evolution of the centres of libration as a function of the Jacobi constant, $C_{\rm J}$, and that the treatment of individual resonances leads to an underestimate of the extent of chaotic regions arising from resonance overlap.

The work presented in Paper I was part of Project CRISS-CROSS (Chaotic Regions of the Inner Solar System – Chaotic Regions of the Outer Solar System). Here we present further results from this project, part of which involved extensive numerical integrations of the full equations of motion of the circular restricted problem (Winter & Murray 1994a,b). In this paper we are concerned with the main features of the phase space for the region *exterior* to the perturber; in particular we are interested in the phenomenon of asymmetric libration which can occur at several exterior resonances. In the next section we describe this unusual phenomenon, give an outline of the analytical theory, and summarize previous work on this subject. In Sect. 3 we present several Poincaré surfaces of section which illustrate the difference between symmetric and asymmetric libration for sample first-, second-, third-, and fourth-order exterior resonances. In Sect. 4 we follow the evolution of the 1:2 resonance as a function of the Jacobi constant using Poincaré surfaces of section to show how the phase space changes. Numerical results derived from the integration of three sample trajectories in the vicinity of the 1:2 resonance are shown in Sect. 5. Our conclusions and a discussion of possible applications are presented in Sect. 6.

2. Asymmetric periodic orbits

In Paper I we introduced what we called Andoyer's Hamiltonian (Eq. (63) of Paper I). This is a Hamiltonian which gives rise to one, two or three equilibrium points, all of which are located where the resonant argument, ψ, is equal to 0 or π. Therefore libration (stable or unstable) always occurs about the line of apses and consequently we can label the interior resonances as *symmetric*. The Hamiltonian considered in Paper I contained a term in $\cos\psi$ but no terms in multiples of the resonant argument. However, the higher order terms in the particle's eccentricity, e, associated with multiples of the resonant argument have to be included when convergence of the expansion of the disturbing function is a problem. This can occur in dynamical studies of the outer regions of the asteroid belt and/or when large eccentricities are involved. In his work on the motion of Hecuba-type asteroids (those librating in the 2:1 interior Jovian resonance) Andoyer (1903) considered terms in the expansion of the disturbing function up to and including second order in e; this meant that he had to include terms associated with $\cos 2\psi$.

Consider the problem of two bodies moving in circular orbits about their common centre of mass. Let the masses of the primary and secondary be m_1 and m_2 respectively. A test particle orbits m_1 with perturbations from m_2, although it affects the motion of neither of the two masses; all motion is confined to the orbital plane of the m_1–m_2 system. Let a, e, ϖ and λ denote the semimajor axis, eccentricity, longitude of periapse, and mean longitude of the particle, respectively. The relevant orbital elements of m_2 are its semimajor a', and its mean longitude λ'. In his study of the interior resonance Andoyer used a Hamiltonian of the form

$$\mathscr{H} = \frac{-\mu_1^2}{2(\Phi + j_1\Psi)^2} - j_2\Psi - \Phi - \mu_2 K_1 \cos\psi - \mu_2 K_2 \cos 2\psi \quad (1)$$

where j_1 and j_2 are integers, $\mu_1 = \mathscr{G}m_1$, $\mu_2 = \mathscr{G}m_2$, $K_1 = ef_1$, $K_2 = e^2 f_2$ (where f_1 and f_2 are functions of Laplace coefficients) and

$$\Phi = \sqrt{\mu_1 a}\left\{\frac{j_1\sqrt{1-e^2} - j_2}{j_1 - j_2}\right\} \quad (2)$$

$$\Psi = \sqrt{\mu_1 a}\left\{\frac{1-\sqrt{1-e^2}}{j_1 - j_2}\right\} \quad (3)$$

are the Poincaré resonant momenta (see Paper I) and $\mathscr{G}$ is the gravitational constant. The corresponding resonant coordinates are

$$\phi = l + \varpi - t \quad (4)$$

$$\psi = j_1 l - j_2(t - \varpi) \quad (5)$$

where $l = \lambda - \varpi$ is the mean anomaly of the particle and t is the time, also equivalent to the mean longitude of the perturber in these units (i.e. $\lambda' = t$). For small values of e the following approximations are valid:

$$\Psi \approx \sqrt{\mu_1 a}e^2/2 \quad (6)$$

$$\Phi \approx \sqrt{\mu_1 a}(1 + j_1 e^2/2) \quad (7)$$

For this Hamiltonian at the 2:1 interior resonance Andoyer used $j_1 = 1$ and $j_2 = 2$. He found that the inclusion of the $\cos 2\psi$ (second order harmonic) terms in the Hamiltonian led to the appearance of *asymmetric* periodic orbits, i.e. resonant orbits with the centre of resonance at neither $\psi = 0$ nor $\psi = \pi$.

Message (1958) conducted a search for asymmetric periodic orbits associated with first-order resonances with Jupiter taking into account the effects of harmonics up to ninth-order. His results indicated that there are, in fact, no asymmetric periodic orbits for the first-order, interior resonances and that Andoyer's result was a consequence of the inclusion of just the first- and second-order harmonics. This result was confirmed and also extended to higher-order resonances by a comprehensive survey of Poincaré surfaces of section for the mass ratio of 10^{-3} in the region interior to the orbit of the perturber (see the plots in Winter & Murray 1994a).

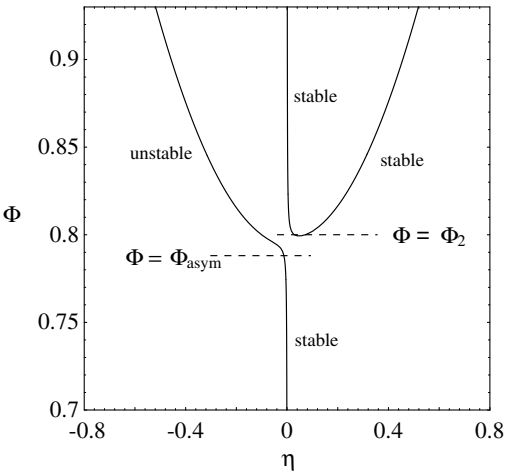

Fig. 1. Diagram of the value of η for the stable and unstable equilibrium points for the Hamiltonian given by Eq. (1) for the 1:2 resonance ($j_1 = 2$, $j_2 = 1$) where the resonant argument ψ is equal to 0 or π.

In the case of exterior resonances the situation is quite different. Consider the Hamiltonian given in Eq. (1) for the 1:2 rather than the 2:1 resonance. In this case $j_1 = 2$ and $j_2 = 1$. A similar analysis can also be carried out for other resonances. Here we make use of the coordinates $\xi = \sqrt{2\Psi}\sin\psi$ and $\eta = \sqrt{2\Psi}\cos\psi$ previously adopted in Paper I. Fig. 1 shows a diagram of the dependence of the η value on Φ for the equilibrium points with $\xi = 0$ for this Hamiltonian; these correspond to points where the resonant argument ψ is equal 0 or π. Note the similarity between this diagram and that shown in Fig. 5 of Paper I for the Hamiltonian of an interior resonance without the second harmonic. However, there is a fundamental difference between the sets of equilibrium points for these two Hamiltonians that is not apparent from an inspection of the diagrams: At a certain value of $\Phi = \Phi_{\rm asym}$ the stable equilibrium point represented by the left-hand branch in Fig. 1 bifurcates such that for $\Phi > \Phi_{\rm asym}$ the curve corresponds to an unstable point and two new stable points appear. These points cannot be represented in the diagram because they are no longer in the $\xi = 0$ plane. Therefore at the equilibrium points ψ is different from 0 or π. Such points give rise to asymmetric periodic orbits and we call this an asymmetric resonance.

Fig. 2 shows the contours of constant $\mathscr{H}$ on surfaces of constant Φ for the 1:2 resonance; these plots allow us to consider the evolution of the asymmetric families of orbits as a function of Φ. Since $\Psi \propto e^2$, the definitions of ξ and η imply that a radial distance in the ξ–η plane is directly proportional to the particle's eccentricity, and the angular position of a point corresponds to the value of the resonant angle, $\psi = 2\lambda - \lambda' - \varpi$. The overall picture is similar to that given in Fig. 4 of Paper I except for the effects of the bifurcation described above. When $\Phi < \Phi_{\rm asym}$ (Fig. 2a) there is only one stable equilibrium point, at $\psi = \pi$, corresponding to the normal situation prior to the bifurcation. As the value of Φ is increased this stable point moves to the left, towards higher values of eccentricity, in accordance with the be-

haviour of the left-hand branch of the curve shown in Fig. 1. For the curves in Fig. 2b, $\Phi > \Phi_{\rm asym}$; this means that the equilibrium point has reached an eccentricity larger than the minimum needed for the bifurcation to occur and has became unstable. There are two new families of orbits, independent from each other, corresponding to librations about the asymmetric resonant orbits. Note that there are also orbits which librate about the three existing equilibrium points in a 'horseshoe' fashion. As Φ increases further (see Figs. 2b–f), we can see that the asymmetric periodic orbits moves towards larger values of eccentricity and also for values of ψ further away from π.

The topology obtained above for the Hamiltonian which includes the first and second harmonics, Eq. (1), does not depend on the resonance considered. Message (1958), as we have already stated, considered a Hamiltonian taking into account the effects of harmonics up to ninth-order. On this basis he found that the exterior 1:2, 2:3 and 3:4 resonances are all asymmetric. He also pointed out a problem with the convergence of the disturbing function in the case of the 3:4 resonance, since asymmetric periodic orbits only arise above a certain threshold value in the eccentricity.

Frangakis (1968, 1973a,b) conducted a numerical exploration of periodic orbits in exterior resonance with Jupiter using a numerically averaged Hamiltonian, i.e. a Hamiltonian where only long-period terms are included. He produced contour plots equivalent to those shown in Fig. 2, finding that the resonances with $\psi = (p+q)\lambda - p\lambda' - q\varpi$ for $p = 1$ and $q = 1, 2, 3, 4$ are all asymmetric. By analysing the existence of the periodic orbits in asymmetric resonance he computed separately the mean values of the direct and indirect parts of the disturbing function showing that only for $p = \pm 1$ would it be possible to have an asymmetric solution to the long-period (averaged) problem.

Message (1970) showed that a bifurcation of a series of asymmetric periodic orbits of the second kind from a series of symmetric ones implies a zero of $\partial^2 \mathscr{H}^{\#}/\partial\psi^2$, where $\mathscr{H}^{\#}$ is the long-period part of the Hamiltonian function (where the Hamiltonian was also averaged numerically). Message (1970) and Message & Taylor (1978) found the values of the eccentricity for which the bifurcation occurs for the resonances with $p = 1$ and $q = 1, 2, 3, \ldots, 7$. They also found that for a very large value of eccentricity, typically $e > 0.95$, there is another bifurcation with the same series of symmetric periodic orbits. Taylor (1981) studied the problem of horseshoe periodic orbits in the 1:1 resonance (the case where $p = \pm 1$ and $q = 0$) for the Sun–Jupiter system and found asymmetric periodic orbits in these resonances.

Fundamental work on this subject was done by Bruno (1976, 1994). He studied the generating orbits (i.e. the limit $\mu_2 \to 0$) searching for many different resonances. He found that asymmetric resonances exist only for the $1 : n$ cases, and that this family is closed and intersects the family of periodic orbits twice (except for the case $n = 1$).

Beaugé (1994) studied the exterior 1:3, 1:2, 2:3 and 3:4 resonances. The problem was treated using two methods. In the first, he used a numerical approach similar to that by Frangakis (1968) and found that the 1:2 and 1:3 resonances are asymmetric while the 2:3 and 3:4 resonances are not. Secondly, he considered Andoyer's Hamiltonian containing the terms with the first and second harmonics of the resonant argument, as in Eq. (1). However, in the case of the 1:3 resonance he took $K_1 = e^2 f_1$ and $K_2 = e^4 f_2$, the terms appropriate to the first- and second-order harmonics of a second order resonance. Using the same kind of approximation adopted in the second fundamental model of resonance (see Henrard & Lemaître 1983, and the summary in Winter & Murray 1996), he found that all four resonances were asymmetric. Beaugé explained that the reason for the disagreement between the two approaches for the 2:3 and 3:4 resonances is due to the problem of convergence of the disturbing function, the same problem as detected by Message (1958) at the 3:4 resonance and clarified by Frangakis (1968).

3. Examples of external libration

Our computation of Poincaré surfaces of section covered in great detail a wide range of interior resonance (from the 3:1 to the 4:3; Winter & Murray 1994a) and exterior resonances (from the 3:4 to the 1:3; Winter & Murray 1994b) for a specific mass ratio. Since these computation were based on the numerical integration of the full equations of motion, our results for symmetric/asymmetric resonances are not dependent on an analytical model. Below we give a series of numerical examples of symmetric and asymmetric libration at first-, second-, third-, and fourth-order exterior resonances. In these and subsequent surfaces of section in this paper we have plotted x and $\dot{x}$ whenever $y = 0$ and $\dot{y} < 0$. Note that the sign of $\dot{y}$ is opposite to that used in the surfaces of section in Paper I. The ambiguity in the sign is a consequence of the relationship between the Jacobi constant and the position and velocity components. Using the equations of motion given in paper I but applied to exterior orbits would result in non-Newtonian motion if $\dot{y}$ is chosen to be positive for prograde orbits.

In the case of interior resonances the location of the centre of any resonance is always at 0 or π. This implies that any trajectory librating about a resonance produces a Poincaré surface of section that has a set of islands symmetric about the line $\dot{x} = 0$ in the x–$\dot{x}$ plane (see the sample of plots in Winter 1994, or the complete set in Winter & Murray 1994a). However, that is not always the case for exterior resonances. Below we show the Poincaré surfaces of section for a representative sample of trajectories in exterior resonances. In Figs. 3, 4, 5 and 6 we compare the surfaces of section of trajectories in symmetric libration with trajectories in asymmetric libration in a different resonance of the same order. For first-order resonances, a trajectory produces a single island in a surface of section; we show the symmetric 2:3 resonance and the asymmetric 1:2 resonance in Figs 3a and 3b respectively. For second-order resonances, there are two islands, and we show the symmetric 3:5 resonance and the asymmetric 1:3 resonance in Figs. 4a and 4b respectively. In the case of third-order resonances, there are three islands, and we show the symmetric 2:5 resonance and the asymmetric 1:4 resonance in Figs. 5a and 5b respectively. Finally, for fourth-order resonances, a trajectory produces four islands in a

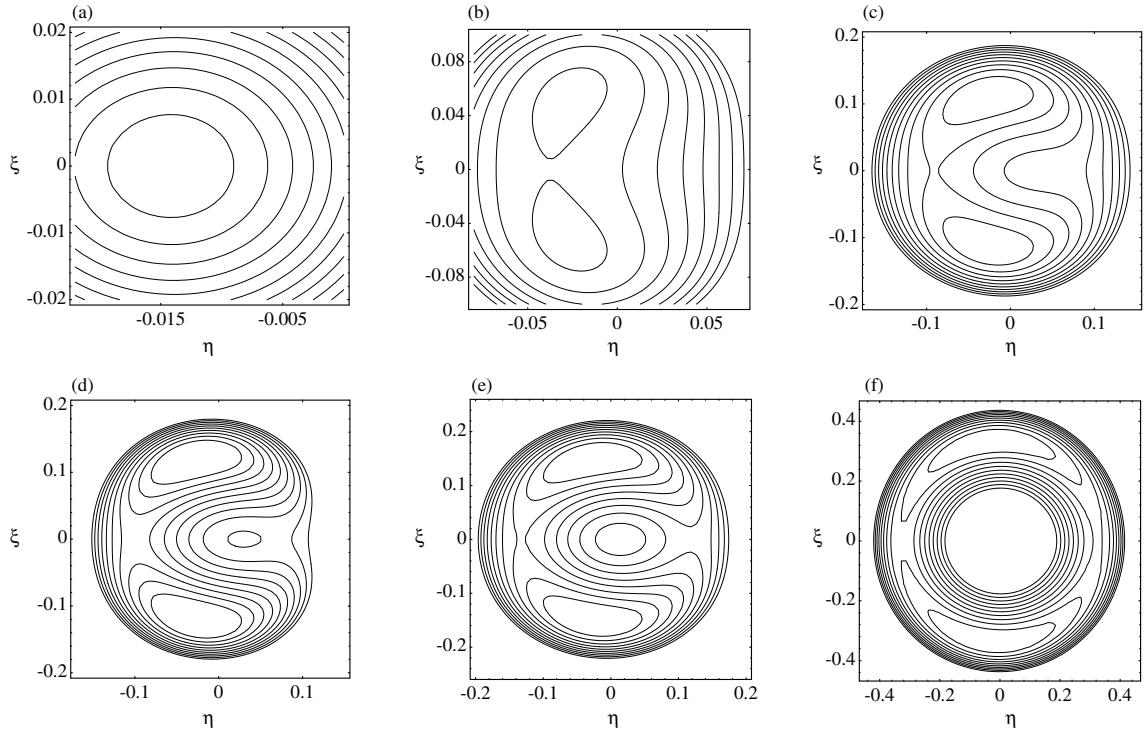

Fig. 2a–f. Contours of constant Hamiltonian (from Eq. (1) with $j_1 = 2$ and $j_2 = 1$) plotted in terms of $\xi = \sqrt{2\Psi}\sin\psi$ and $\eta = \sqrt{2\Psi}\cos\psi$ for the cases **a** $\Phi < \Phi_{\rm asym}$, **b** $\Phi_{\rm asym} < \Phi < \Phi_1$, **c** $\Phi \approx \Phi_1$, **d** $\Phi_1 < \Phi < \Phi_2$, **e** $\Phi_2 < \Phi$, and **f** $\Phi_2 \ll \Phi < \sqrt{\mu_1}$. Note the differences in scale of the diagrams.

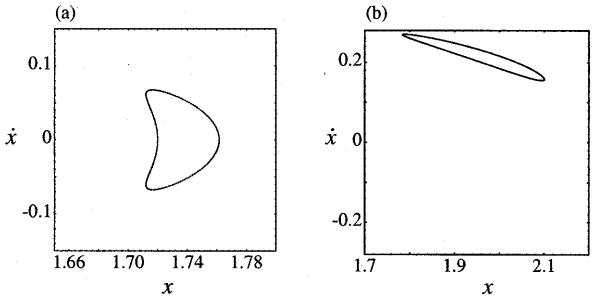

Fig. 3a and b. Poincaré surfaces of section of orbits librating in first-order resonances. **a** The single island associated with symmetric libration in the 2:3 resonance. **b** The single island associated with asymmetric libration in the 1:2 resonance.

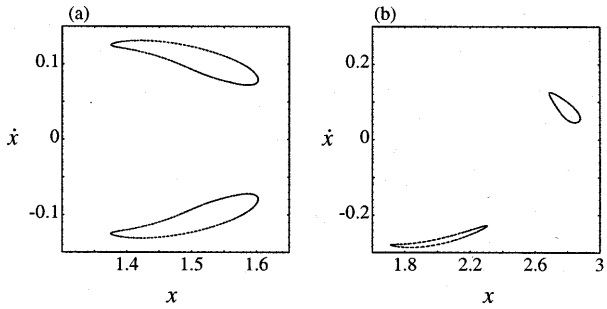

Fig. 4a and b. Poincaré surfaces of section of orbits librating in second-order resonances. **a** The two islands associated with symmetric libration in the 3:5 resonance. **b** The two islands associated with asymmetric libration in the 1:3 resonance.

surface of section, and we show the symmetric 3:7 resonance and the asymmetric 1:5 resonance in Fig. 6a and 6b respectively. It is interesting to note that for the range of a and e considered in our numerical survey, only the resonances of the form $1{:}m$, where $m = 2, 3, 4, 5$, are found to be asymmetric; this agrees with the numerical work of Beaugé (1994). All the other resonances located between the 3:4 and 1:5 resonances are found to be symmetric in our study.

From the definition of the Jacobi constant and the equations of motion expressed in terms of the rotating coordinate system (see Eqs. (1)–(3) of Paper I) it is clear that if $(x, \dot{x})$ denotes a point on the surface of section, then the point $(x, -\dot{x})$ must also lie on the same surface. Consequently, all the islands generated from a trajectory in asymmetric libration with $\psi = \psi^*$ will have a 'mirror' image generated from a different trajectory in asymmetric libration at the same resonance and with the same amplitude of libration but with $\psi = -\psi^*$. This explains the obvious symmetry of the Poincaré surfaces of section about the x-axis for the trajectories shown in Winter (1994) and in Winter & Murray (1994b).

We have already remarked on the fact that as the value of Φ increases, the centre of libration moves to larger values of the eccentricity while the resonant angle also changes. Fig. 7 shows the evolution of the resonant angle with respect to the

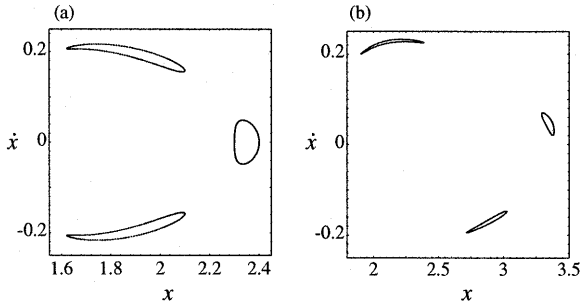

Fig. 5a and b. Poincaré surfaces of section of orbits librating in third-order resonances. **a** The three islands associated with symmetric libration in the 2:5 resonance. **b** The three islands associated with asymmetric libration in the 1:4 resonance.

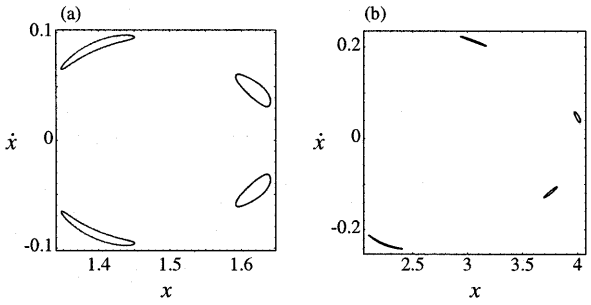

Fig. 6. Poincaré surfaces of section of orbits librating in fourth-order resonances. **a** The four islands associated with symmetric libration in the 3:7 resonance. **b** The four islands associated with asymmetric libration in the 1:5 resonance.

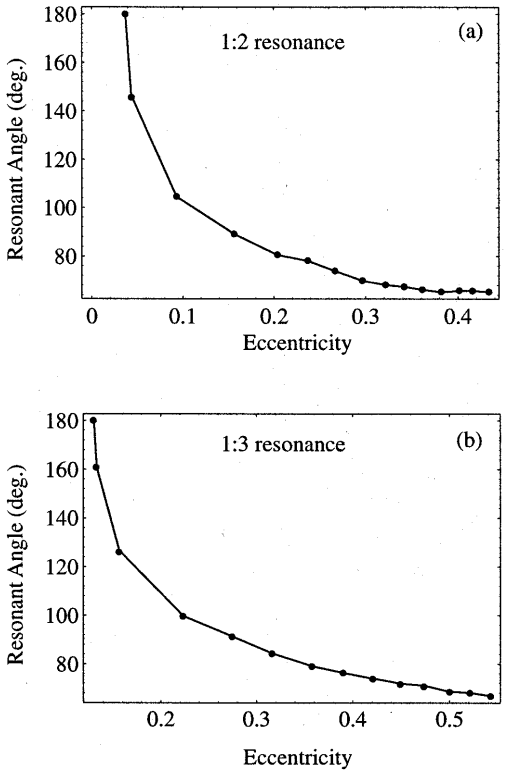

Fig. 7a and b. The relationship between the resonant angle, ψ, at the centre of libration and the eccentricity, e, for **a** the 1:2 and **b** the 1:3 exterior resonances.

eccentricity for the centre of the 1:2 and 1:3 resonances. Both results are in good agreement with those from Beaugé (1994).

4. Numerical results

In this section we follow in some detail the evolution of the orbits associated with the asymmetric 1:2 resonance through a range of twelve values of the Jacobi constant, C_J, between 2.90 and 3.15 (see Figs. 8–19). A similar study can be achieved for the 1:3 and other external resonance using the plots given in Winter & Murray (1994b). The purpose of the present study is to show in detail (i) how asymmetric libration arises in the context of the full, non-averaged problem, (ii) the actual extent of the islands associated with libration at the 1:2 resonance, and (iii) the chaotic nature of the phase space associated with external resonances.

The data for the plots shown below were derived from the results of the extensive integrations carried out by Winter & Murray (1994b). For each of 366 values of the Jacobi constant, Winter & Murray (1994b) produced a surface of section containing several hundred repesentative starting values. For the current paper we restrict ourselves to a study of parts of only twelve of these surfaces of section. Note that a 'line' of points is sometimes visible along the x-axis of some surfaces of section. These represent the initial positions of trajectories which invariably became chaotic but leave evidence of the regular spacing of their starting values.

Fig. 8 shows the Poincaré surface of section for the lowest Jacobi constant considered in our survey. In this plot we have (from left to right) a family of single islands due to the 3:4 resonance (centred at $x \approx 1.62$), a family of single islands due to the 2:3 resonance (centred at $x \approx 1.75$), and finally, two families of single islands (one for $\dot{x} > 0$ and other for $\dot{x} < 0$) due to the asymmetric 1:2 resonance (centred at $x \approx 1.96$). Note that the rest of the phase space is mostly chaotic and that the two branches of the 1:2 resonance are separated by an extensive chaotic region. At this stage the two independent periodic orbits in the 1:2 resonance have a high eccentricity ($e \approx 0.43$) and the resonant angle has the largest difference from π with $\psi \approx \pm\pi/3$. As the Jacobi constant increases the eccentricity decreases and the resonant angle moves towards π. This is also shown in Fig. 7a. From Figs. 8–11 we can see that the size of the libration regions about the stable points corresponding to the periodic orbits in the 1:2 resonance are growing as C_J increases. This means that the maximum amplitudes of libration are also increasing and that the chaotic region between is decreasing. Note that secondary resonances can also appear around asymmetric resonances (see Fig. 11).

The birth of orbits that librate about the two families of asymmetric librations is shown in Figs. 12–15. In Fig. 12 there is a darker area where the density of points is larger than in the rest of the plot; this corresponds to the broad separatrix that

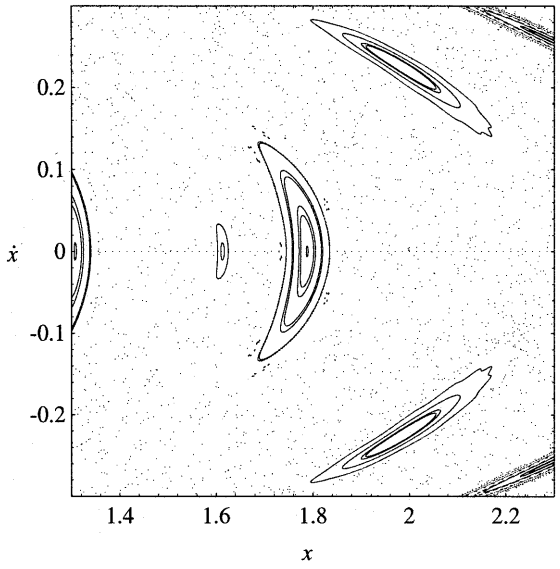

Fig. 8. Poincaré surface of section for $C_J = 2.900$

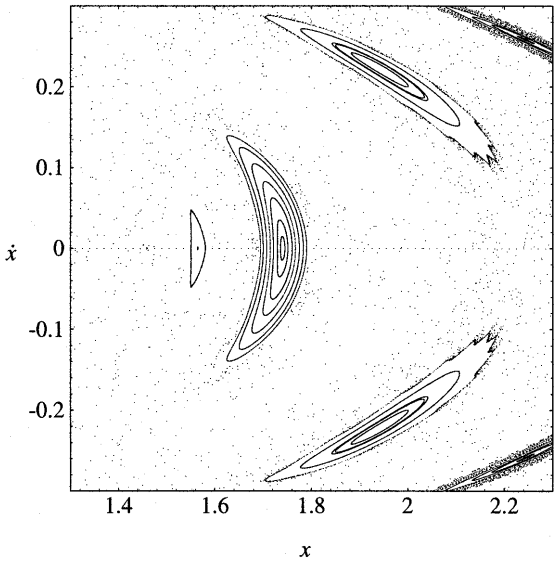

Fig. 9. Poincaré surface of section for $C_J = 2.930$

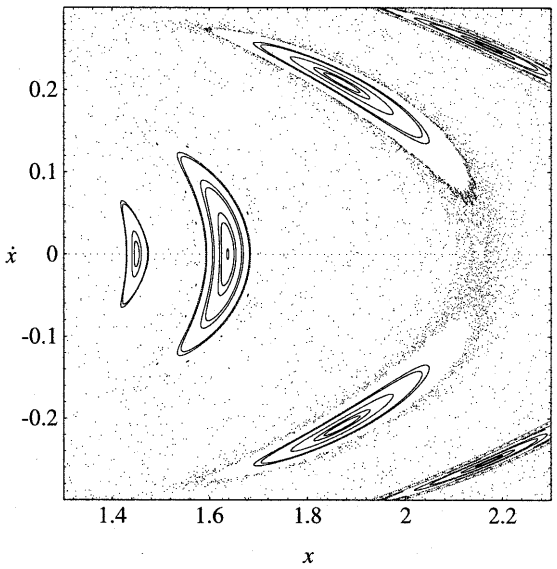

Fig. 10. Poincaré surface of section for $C_J = 2.983$

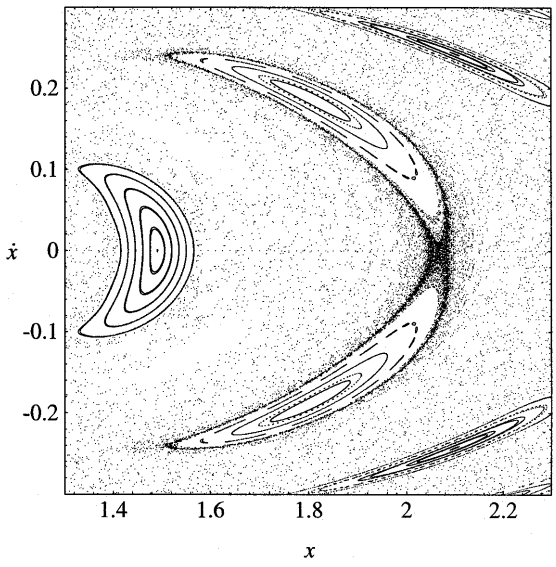

Fig. 11. Poincaré surface of section for $C_J = 3.033$

passes through the unstable region where the resonant angle is equal to π. This region starts to show some structure as the value of the Jacobi constant increases (Figs. 13 and 14). In Fig. 15 the structure is well defined and corresponds to regular trajectories librating about the 1:2 resonance with a much larger amplitude of libration (equivalent to that found for libration about the interior 2:1 resonance). This libration involves all three equilibrium points. Note that now the separatrix has become well defined.

Various stages of the evolution of the asymmetric 1:2 resonance for small eccentricities ($e < 0.2$) are shown in Figs. 16–19. The topology of the phase space defined by this sequence of plots is in good agreement with the topology inferred from Fig. 2 derived from Andoyer's Hamiltonian. This is not surprising since we are now reaching a regime where an expansion to second order in the eccentricity provides a sufficiently good representation. In Fig. 16 the first trajectory corresponding to outer circulation has just appeared. Between this orbit and the periodic orbit of the first kind at $x \approx 1.46$ there is no extensive chaotic region, although it is likely that several smaller ones may exist. As the Jacobi constant increases the outer circulation region becomes much larger (see Fig. 17). At a certain stage the periodic orbit of the first kind disappears, but there are still asymmetric periodic orbits (see Fig. 18). Then, in the final stage, when the eccentricity gets so small that the three equilibrium points coalesce, there remains just one stable equilibrium point at $\psi = \pi$ (see Fig. 19).

The work presented in this section in combination with that presented in Winter & Murray (1994a,b) permits us to make some important comparisons. If we compare the asymmetric

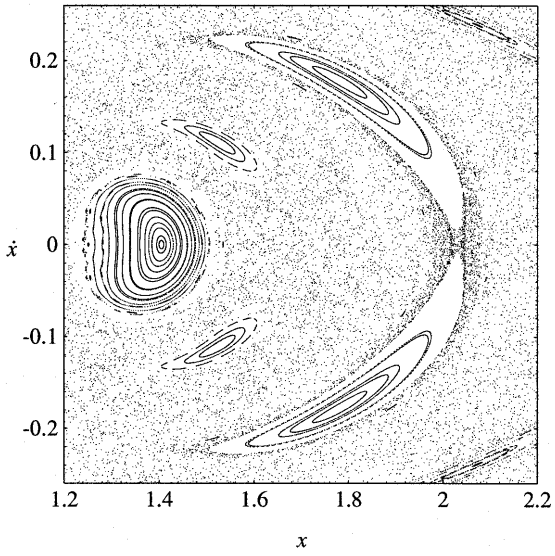

Fig. 12. Poincaré surface of section for $C_J = 3.050$

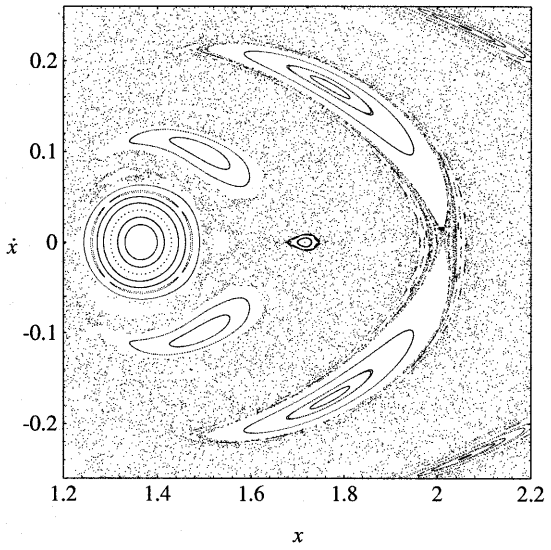

Fig. 13. Poincaré surface of section for $C_J = 3.059$

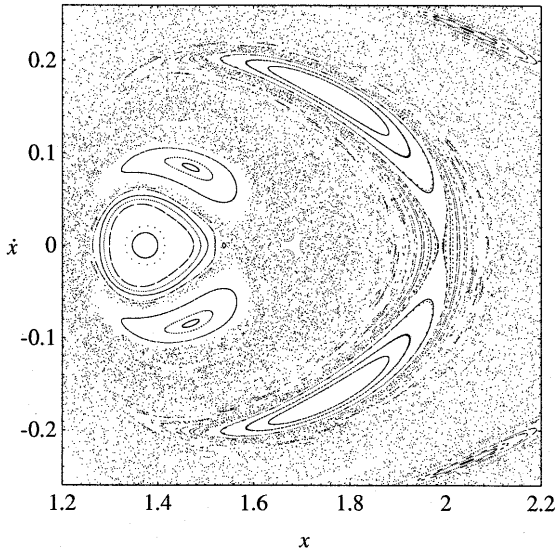

Fig. 14. Poincaré surface of section for $C_J = 3.069$

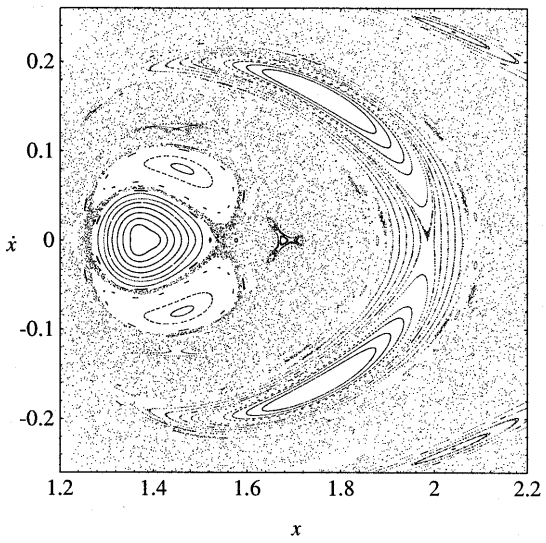

Fig. 15. Poincaré surface of section for $C_J = 3.070$

exterior resonances with their corresponding symmetric interior ones (for example the 1:2 with the 2:1) we note that the former have an additional separatrix dividing what would be the entire regular area of libration into two independent regular areas divided by a sometimes extensive chaotic separatrix. Furthermore, the maximum amplitude of libration for a particle in the asymmetric 1:2 resonance would be less than half that of the equivalent amplitude for the symmetric 2:1 resonance. Therefore, in terms of surface area in the x–$\dot{x}$ plane, regular libration in the combined areas of both branches of the 1:2 exterior resonance is less than that of the 2:1 interior resonance. The same applies to other external resonances. On this basis alone we can conclude that the region exterior to the perturbing mass is likely to be more chaotic than the interior region; this seems to be confirmed by a comparison of surfaces of section for the same value of the Jacobi constant.

5. The 1:2 resonance

In this section we show the evolution of various orbital parameters for three trajectories in order to illustrate the types of libration that can occur in $1 : n$ resonances. Although similar plots can be obtained for other, we choose to follow motion at the 1:2 resonance since this is the simplest external resonance that exhibits asymmetric libration. In each of the following plots (Figs. 20–22) we show: (a) the time variation of the semimajor axis a, eccentricity, e, longitude of the pericentre, ϖ and the resonant argument, $\varphi = 2\lambda - \lambda' - \varpi$, (b) the equivalent Poincaré surface of section, and (c) the quantities η and ξ plotted as Cartesian coordinates. In the case of the plots of the semimajor axis (the uppermost sub-plot in Figs. 20a, 21a and 22a) we indicate the location of the nominal resonant semimajor axis at $a = 1.587$ by a dashed line. The limits on the orbital element plots are the

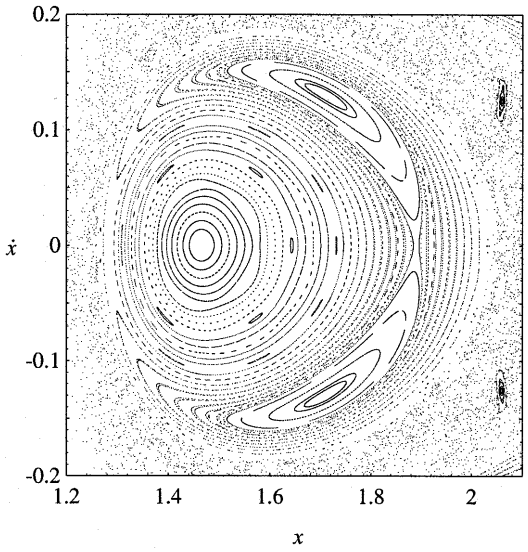

Fig. 16. Poincaré surface of section for $C_J = 3.104$

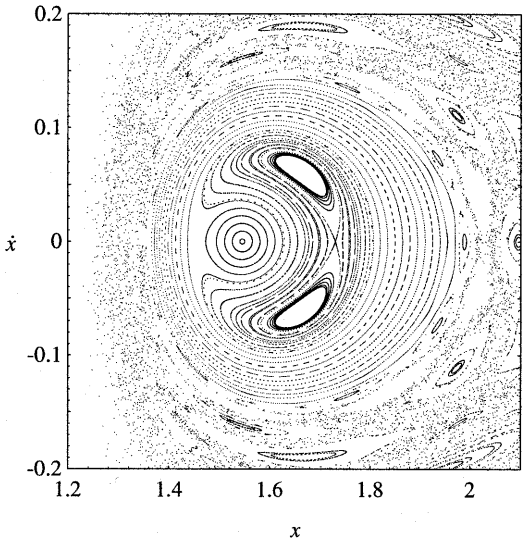

Fig. 17. Poincaré surface of section for $C_J = 3.140$

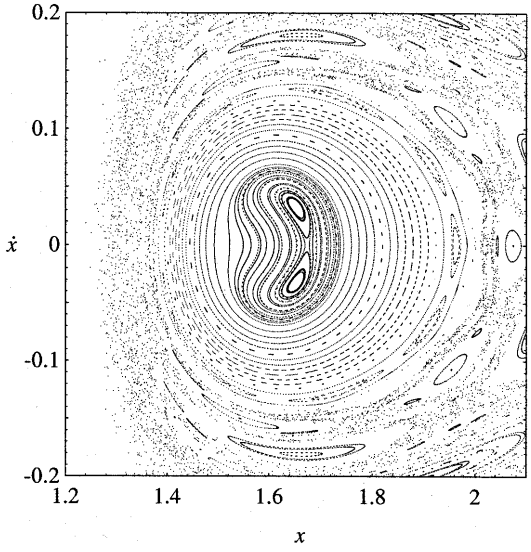

Fig. 18. Poincaré surface of section for $C_J = 3.147$

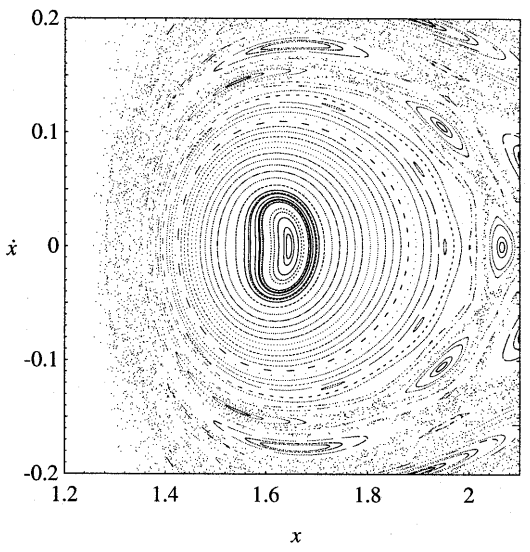

Fig. 19. Poincaré surface of section for $C_J = 3.150$

same in each case. The plots of orbital elements and the variation in ξ and η are derived from integrations of 150 orbital periods of the perturber (the time units in the plots of orbital elements).

For each trajectory we have taken $C_J = 3.07$; this corresponds to the value used in the surface of section plots shown in Fig. 15. It is important to note the similarity between the ξ–η plots and some of the ξ–η curves shown in Fig. 2. However, the contours shown in Fig. 2 are the paths in ξ–η space that a particle would follow *if* its motion could be described by the Hamiltonian given in Eq. (1) for the 1:2 resonance, while the ξ–η plots in Figs. 20–22 are derived from an integration of the full equations of motion. The fact that there is such a striking similarity between the curves and plots shows the ability of the resonant Hamiltonian to reflect at least some aspects of the actual motion of the particle. The 'roughness' of the ξ–η plots in Figs. 20–22 shows the effect of additional perturbations not associated with simple 1:2 resonance.

Fig. 20 shows an example of a large amplitude, symmetric libration about both centres of asymmetric libration. The starting conditions were $x = 2$ and $\dot{x} = 0.04$. Note from the φ and ξ–η plots that the regular libration is about π with an amplitude of $\sim 145°$. The plot of semimajor axis in Fig. 20a shows clear variation of a across the nominal resonant value. It is easy to show that $\dot{a}$ and $\dot{e}$ have the same sign for exterior, first-order resonances; this explains the overall similiarity in the behaviour of a and e plots. There is only a slight regression of the pericentre.

Keeping the same Jacobi constant and initial $\dot{x}$ of 0.04 but changing the the initial x to 1.98 produces a clear example of asymmetric libration with an amplitude of $\sim 60°$ (see Fig. 21), although the centre of the libration (exact asymmetric reso-

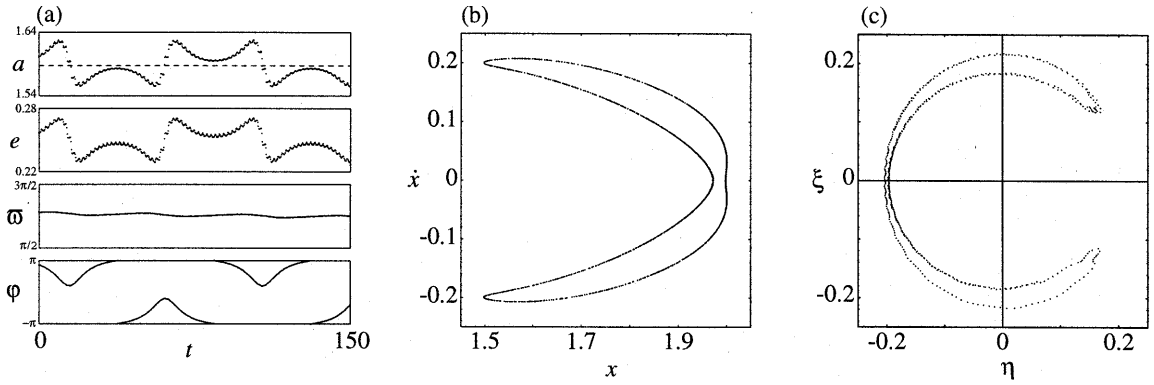

Fig. 20. a Variation of orbital elements, **b** surface of section and **c** the ξ and η plot illustrating large amplitude symmetric libration at the 1:2 resonance.

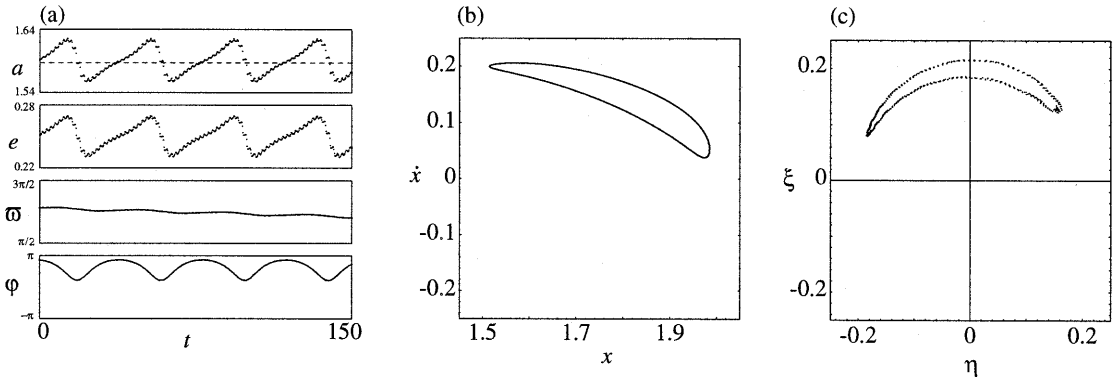

Fig. 21. a Variation of orbital elements, **b** surface of section and **c** the ξ and η plot illustrating large amplitude asymmetric libration at the 1:2 resonance.

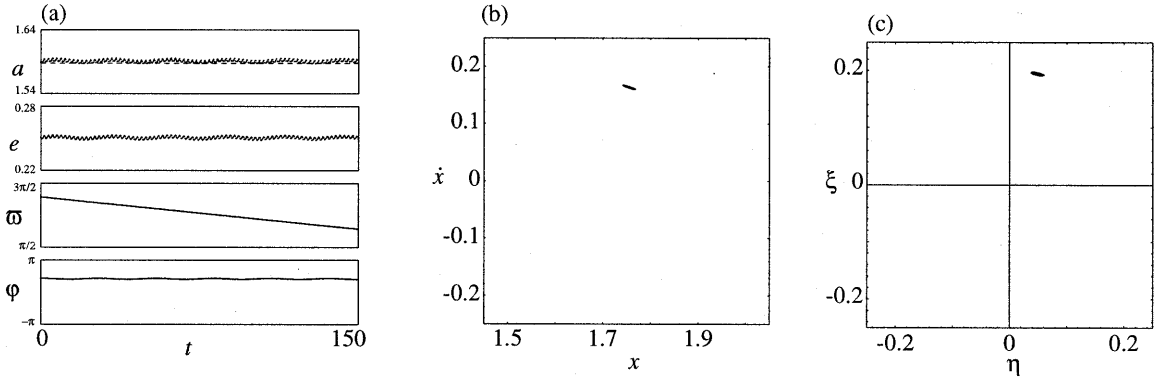

Fig. 22. a Variation of orbital elements, **b** surface of section and **c** the ξ and η plot illustrating asymmetric libration close to the exact centre of 1:2 resonance.

nance) is difficult to determine from this plot alone. Note that ϖ has a larger regression rate than that for the symmetric libration shown in Fig. 20.

Fig. 22 shows the result of choosing starting conditions ($x = 1.767$, $\dot{x} = 0.16$) close to the centre of the asymmetric libration at $\varphi \approx 76°$. Here the libration amplitude is small ($\sim 3°$) and there is little variation in semimajor axis and eccentricty. However, the longitude of pericentre is regressing at a large, constant rate. The fact that the semimajor axis lies close to but above the value associated with the nominal resonant location reflects the fact that the pericentre regression has caused a small outward shift in the value of the exact resonance.

Since we have used the same value of the Jacobi constant for each trajectory, we can superimpose the three surfaces of section shown in Fig. 20b, 21b and 22b. By using negative values of $\dot{x}$ in the starting conditions for the trajectories shown in Figs. 21 and 22 we could have plotted the other branch of the 1:2 asymmetric libration. However, it is important to remember that even though this would have exactly the same value of the Jacobi constant and

even approximately the same value of the resonant Hamiltonian, this would have been a separate trajectory.

6. Conclusions and discussion

In this paper we have attempted to carry out a survey of the origins and evolution of the phenomenon of asymmetric libration at resonances exterior to the perturbing body in the context of the planar, circular, restricted three-body problem. In particular:

- We have confirmed the existence of asymmetric periodic orbits which are associated with exterior resonances of the form $p : p + q$ with $p = 1$ and $q = 1, 2, 3, 4$; there may also be asymmetric resonances associated with higher values of q.
- Using full integrations we have followed the actual evolution of the family of orbits associated with such resonances, with particular attention on the 1:2 resonance. Our results show the bifurcation that generates the asymmetric orbits, the breakdown of the trajectories that librate about the three equilibrium points, and finally the formation of small, isolated islands of stable libration.
- From an examination of the extent of libration at the 1:2, 2:1 and other resonances, and a study of the respective regions of the phase space we conclude that the region exterior to the perturbing mass is more chaotic than the region interior to it.

The existence of asymmetric periodic orbits associated with exterior $1 : n$ resonances is a relatively recent subject and many of the results are not well known. Although Andoyer's original work was an attempt to understand the 2:1 interior resonance (Andoyer 1903), it was motivated by a desire to understand the motion of actual objects— the Hecuba group of asteroids librating at 2:1 resonance. We are unaware of any Solar System 'particles' (in the context of the restricted problem) that are trapped in exterior $1 : n$ resonances with an interior perturbing mass. However, that in itself might be an important clue as to the importance of asymmetric libration in the dynamical evolution of the Solar System.

If the extent of the regular parts of the phase space associated with exterior resonances is indeed more limited that that in interior resonances then from an initially random radial distribution or particles and perturbing masses the chances of a particle being in an asymmetric resonance is smaller than it being in an interior symmetric resonance. Add to that the connected observation of more extensive chaotic regions in the exterior region and it seems plausible that interior resonances would be preferred. For example, asymmetric resonance and chaos may have played an important role in depleting regions immediately exterior to the orbits of the major planets in the early stages of the formation of the Solar System. They could also have had a role in the tidal evolution of planetary satellites where there is no *a priori* reason that $1 : n$ resonances should not have been encountered; in this case a small satellite could be considered as the 'particle' and a larger satellite as the perturbing mass.

Recently, there has been a lot of work published concerning the capture of particles into exterior resonances when considering dissipatives effects like nebular or Poynting–Robertson drag (see for instance Lazzaro et al. 1994, and the references therein). This is another example where the phenomenon of asymmetric resonance might play an important role.

Acknowledgements. We wish to thank Michel Hénon for making us aware of the work of Bruno. Part of this research was funded by the UK PPARC, CAPES (proc. 445/90-1) and CNPq (proc. 520044/95-9).

References

Andoyer M. H., 1903, Bull. Astron. 20, 321
Beaugé C., 1994, Celest. Mech. Dyn. Ast. 60, 225
Bruno A. D. 1976, Preprint of Inst. Appl. Mat. AS USSR No.95
Bruno A. D. 1994, The Restricted 3-Body Problem: Plane Periodic Orbits, Walter de Gruyter, Berlin
Frangakis C. N., 1968, Dissertation, Univ. Liverpool
Frangakis C. N., 1973a, Astrophys. Sp. Sci. 22, 421
Frangakis C. N., 1973b, Astrophys. Sp. Sci. 23, 17
Henrard J., Lemaître A., 1983, Celest. Mech. 30, 197
Lazzaro D., Sicardy B., Roques F., Greenberg R., 1994, Icarus, 108, 59
Message P. J., 1958, AJ 63, 443
Message P. J., 1970, in: Periodic Orbits, Stability and Resonances, ed. G. E. O. Giacaglia, D. Reidel, Dordrecht
Message P. J., Taylor D. B., 1978, in: Dynamics of Planets and Satellites and Theories of their Motion, ed. V. Szebehely, D. Reidel, Dordrecht
Taylor, D. B., 1981, A&A 103, 288
Winter O. C., 1994, The Phase Space of the Circular Restricted Three-Body Problem, Dissertation, Univ. London
Winter O. C., Murray C. D., 1994a, Atlas of the Planar, Circular, Restricted Three-Body Problem. I. Internal Orbits, QMW Maths Notes, London
Winter O. C., Murray C. D., 1994b, Atlas of the Planar, Circular, Restricted Three-Body Problem. II. External Orbits, QMW Maths Notes, London
Winter O. C., Murray C. D., 1996, A&A (in press)

This article was processed by the author using Springer-Verlag LaTeX A&A style file *L-AA* version 3.